

# Site-Specific Evaluation of Bioactive Coumarin-Loaded Dendrimer G4 Nanoparticles against Methicillin Resistant *Staphylococcus aureus*

Ahmed I. Foudah,\* Mohammed H. Alqarni, Samir A. Ross, Aftab Alam, Mohammad Ayman Salkini, and Piyush Kumar



Cite This: *ACS Omega* 2022, 7, 34990–34996



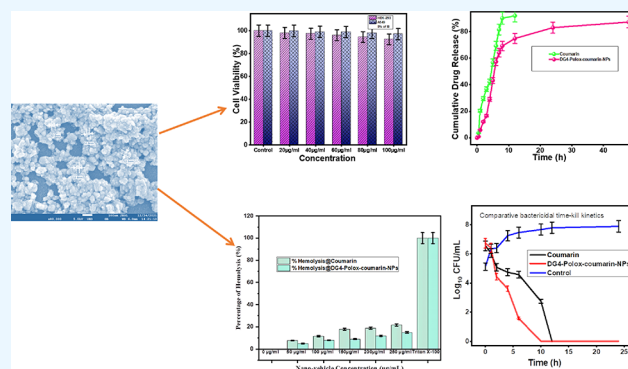
Read Online

ACCESS |

Metrics & More

Article Recommendations

**ABSTRACT:** Methicillin-resistant *Staphylococcus aureus* (MRSA) is a foremost treatment challenge in today's clinical practice. Natural coumarins contain a variety of bioactivities and have the ability to alter resistance in several ways. In developing effective drug delivery methods, the goal is to maximize biocompatibility while minimizing toxicity. With this in mind, this work investigated the site-specific potential of dendrimer G4 poloxamer nanoparticles loaded with bioactive coumarin. The goal of the current work is to deliver a complete evaluation of dendrimer G4 poloxamer nanoparticles against MRSA. Coumarin-loaded dendrimer G4 poloxamer nanoparticles were thoroughly investigated and characterized using various techniques, including particle size, shape, entrapment efficiency, in vitro drug release, hemolysis assay, cytotoxicity, antibacterial activity, and bactericidal kinetics. Studies showed that the newly developed dendrimer G4 poloxamer nanoparticles exhibited significantly lower levels of hemolysis and cytotoxicity. The results showed that the in vitro drug release of coumarin from dendrimer G4 poloxamer nanoparticles was slower compared to coumarin in its free form. This innovative therapeutic delivery technology may enhance the defense of coumarin against MRSA.



## 1. INTRODUCTION

Infections developed by pathogenic bacteria, especially antibiotic-resistant bacteria, are responsible for thousands of pathogenic conditions and deaths and pose a significant public health risk.<sup>1</sup> *Staphylococcus aureus* (*S. aureus*) is one of the furthestmost prevalent life-threatening microorganisms spread through food and causing outbreaks in humans. Penicillin, a beta-lactam antibiotic, is commonly used to alter infections triggered by *S. aureus*. To destroy bacteria, penicillin and other beta-lactam antibiotics interfere with synthesizing bacterial cell walls.<sup>2</sup> After some time, penicillin resistance will develop because the organisms develop beta-lactamase. Other antibiotics, such as penicillinase-stable penicillin and methicillin, have been developed to combat the resistance mechanisms that have developed.<sup>3</sup>

Approximately 60–89% of nosocomial infections are instigated by methicillin-resistant *Staphylococcus aureus* (MRSA). This has resulted in 19,000 deaths and more than \$3 billion in annual spending on health care improvements in the United States alone.<sup>4</sup> MRSA is believed to be directly responsible for more than 11,000 deaths in the United States annually. This is in addition to more than 2,000,000 cases of disease caused by resistant infections yearly.<sup>5</sup> Numerous

therapeutic approaches such as chemotherapy, in which multiple antibiotics are administered in combination, and non-chemotherapeutic approaches have been developed and extensively researched for treating severe MRSA infections. MRSA bacteria are resistant to most beta-lactam antibiotics such as penicillin and cephalosporins<sup>6</sup> and frequently practiced antibiotics, particularly, for instance, erythromycin, clindamycin, gentamycin, ciprofloxacin, and fusidic acid,<sup>7</sup> with further restricting treatment therapy possibilities. Due to its tendency to form biofilms, it is highly resistant to the vast majority of regularly administered antibiotics. Antibiotics, which are used in treating diseases that affect both humans and animals, are commonly shown to be ineffective due to the rapidly increasing antimicrobial resistance (AMR).<sup>8</sup> Then, the effectiveness of antibiotics is slowly decreasing, challenging current research on

Received: June 12, 2022

Accepted: September 9, 2022

Published: September 22, 2022



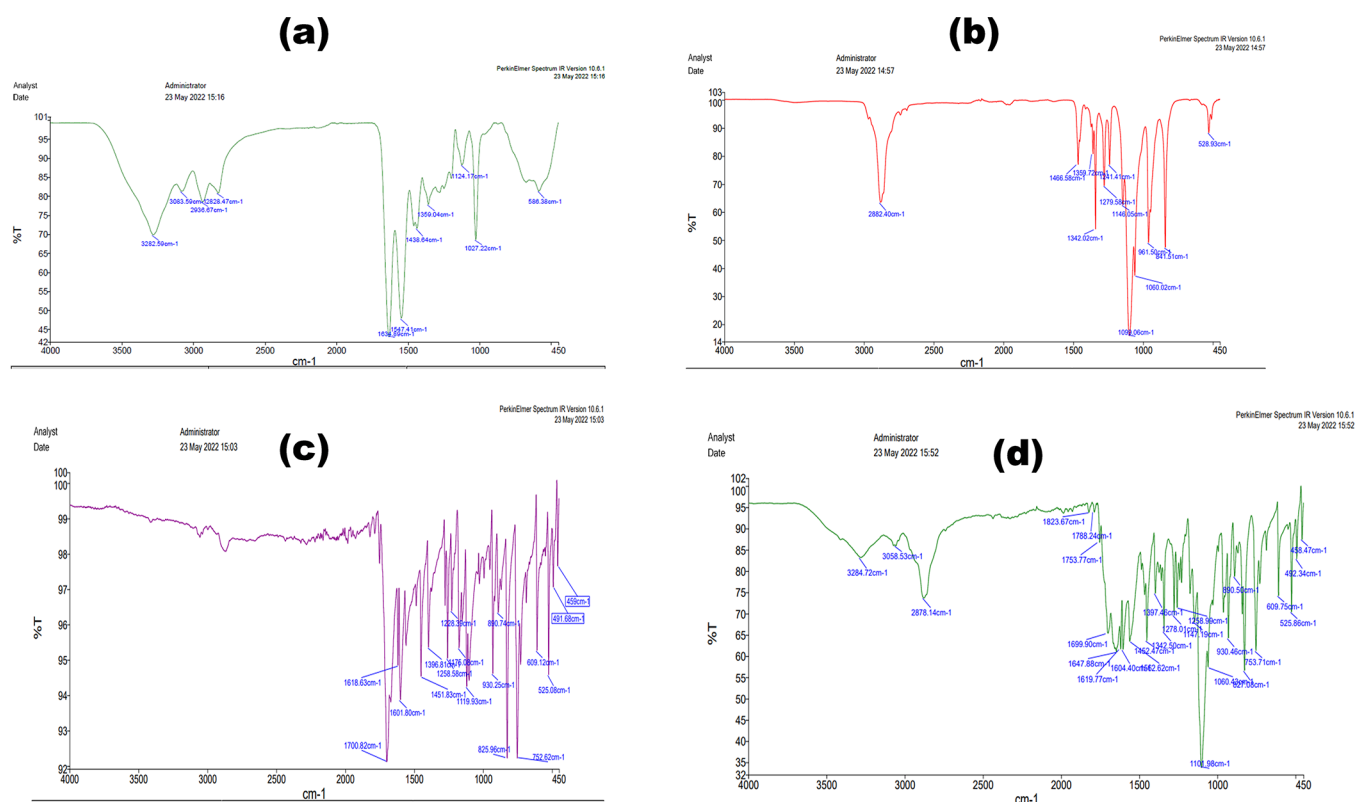


Figure 1. FTIR spectra of (a) PAMAM, (b) poloxamer, (c) coumarin, and (d) PAMAM-poloxamer-coumarin.

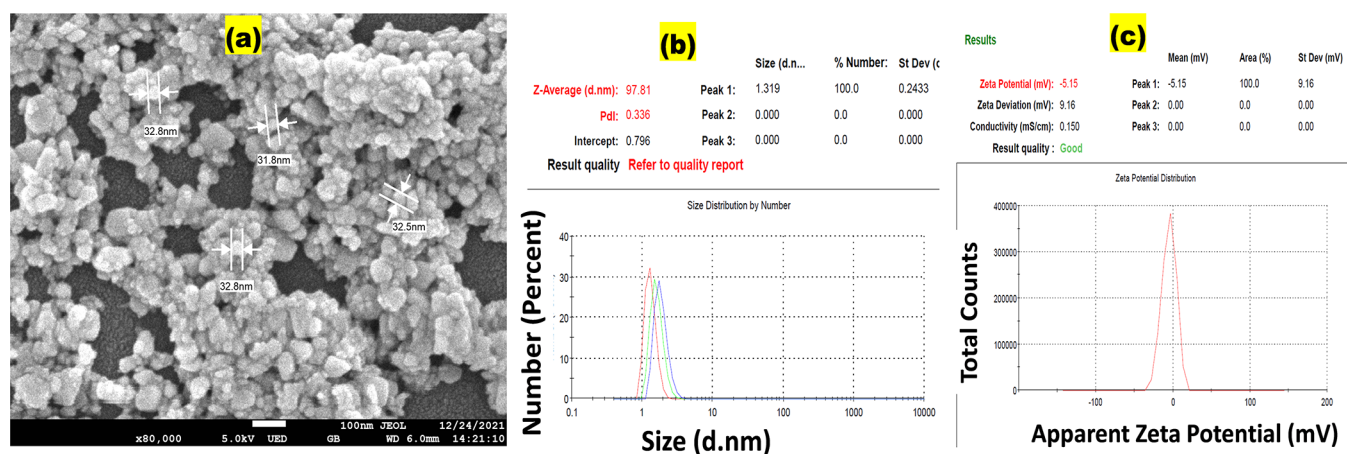


Figure 2. (a) FE-SEM image of DG4-polox-coumarin NPs; (b) characterization of DG4-polox-coumarin by DLS; (c) zeta sizer of DG4-polox-coumarin NPs.

the design of innovative antimicrobial therapies.<sup>9</sup> Antibiotic-resistant bacteria are a major problem worldwide. Today, antibiotic-resistant microorganisms pose a global threat to public health. The increase in antibiotic-resistant bacteria is directly related to the deterioration of clinical care due to the overuse of antibiotics and can cause complications such as pneumonia and acute endocarditis.<sup>10</sup>

Several groups have recently discovered that coumarin and its derivatives have potent activity against various infections, including *S. aureus* and MRSA.<sup>11–16</sup> Based on the available literature, we have chosen coumarin as an antibacterial biofilm agent for developing MRSA nanof ormulation. To combat the problem of antimicrobial resistance, novel approaches using nanodelivery systems are currently being explored. These

approaches have shown the potential to overcome the limitations of conventional delivery systems, such as increased local drug concentration at infection sites, reduced drug exposure at healthy sites, and protection of the drug from premature enzymatic degradation.<sup>17</sup>

In this work, we successfully synthesized two different conjugation ratios of a poloxamer-attached dendrimer G4. In addition, the model drug coumarin was introduced into the hydrophobic interior of the conjugates. The primary purpose of this work was to evaluate dendrimer G4 for its potential as a drug target against MRSA. The chemical and structural adaptability promotes the adoption of biocompatible and biodegradable carriers.

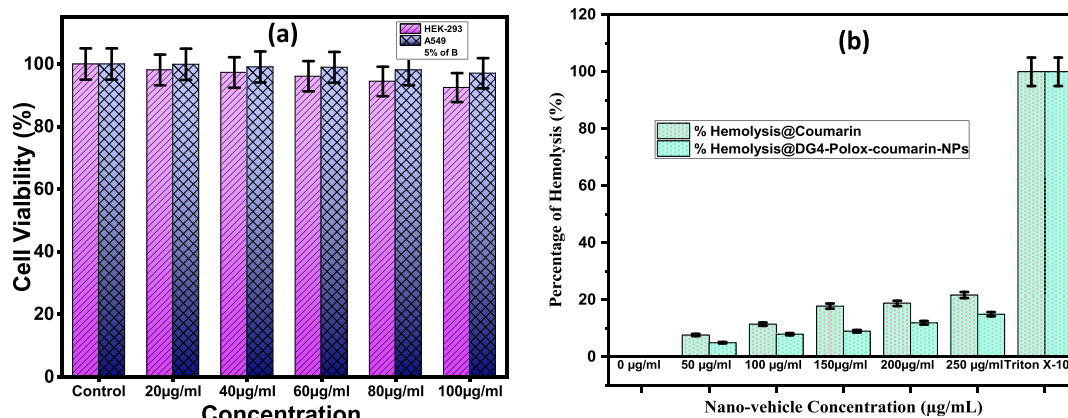


**Figure 3.** (a) Percentage of cell viability after treatment with DG4-polox-coumarin NPs; (b) percentage of hemolytic toxicity profiles of DG4-polox-coumarin NP.

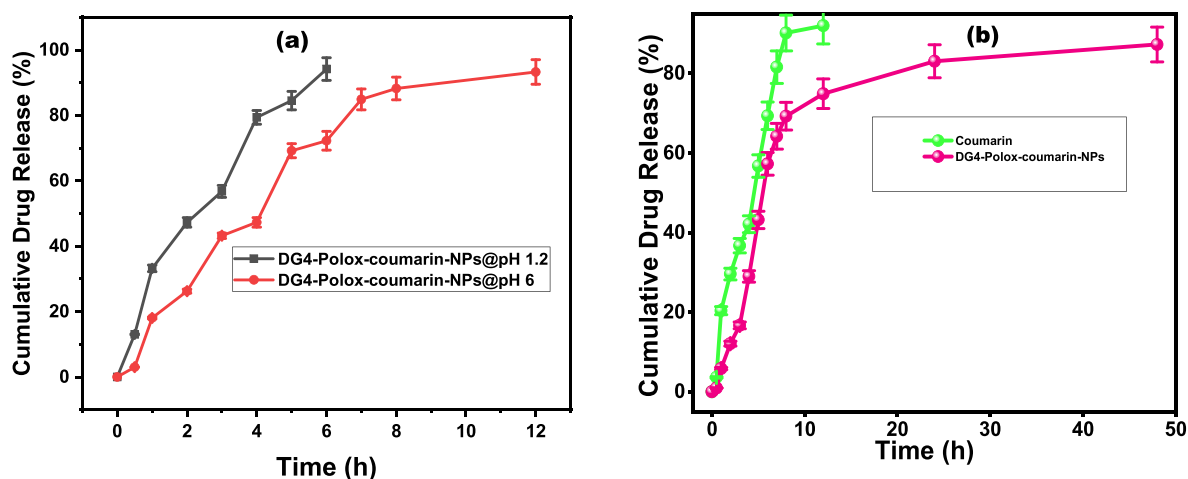


**Figure 4.** In vitro cumulative percentage of the drug release study. (a) DG4-polox-coumarin NP in acidic and neutral pH; (b) bare coumarin and DG4-polox-coumarin NPs.

## 2. RESULTS AND DISCUSSION

**2.1. Compatibility Study.** The results of the characterization studies were used to determine how the spectrum of activity of the coumarin samples would affect product design and development strategies. Coumarin and excipients were subjected to FTIR analysis. The characteristic spectra of coumarin and excipients showed the alkane groups ( $-\text{CH}$ ,  $-\text{CH}_2$ ,  $-\text{CH}_3$ ) stretching at  $2800\text{--}3000\text{ cm}^{-1}$ . The IR spectrum of coumarin shows lactone carbonyl at  $1701\text{ cm}^{-1}$ ,  $\text{C}=\text{C}$  at  $1601\text{ cm}^{-1}$ ,  $1451\text{ cm}^{-1}$ , and  $\text{C}-\text{O}-\text{C}$  at  $1258\text{ cm}^{-1}$ . The broad transmittance band at  $3282\text{ cm}^{-1}$  shows the stretching vibration of the  $-\text{NH}-$  groups of PAMAM; the band at  $1634\text{ cm}^{-1}$  is due to the  $\text{C}=\text{O}$  stretching of carbonyl groups of PAMAM internal amides. The absorption peaks at  $1099\text{ cm}^{-1}$  can be ascribed to the stretching vibration of the  $\text{C}-\text{O}-\text{C}$  groups of poloxamer. The observed bands prove the presence of coumarin and excipient molecules in the sample. The study results indicate no interaction between the drug and excipients, as the FTIR spectrum shows peaks for both components (the drug and excipients). The infrared spectrum of the drug-loaded dendrimer formulation was compared to the standard spectrum of pure coumarin. As shown in Figure 1a–d, the peak associated with a specific functional group, molecule binding, and its presence and absence were identified.

**2.2. Morphology, Particle Size, Polydispersity, and Determination of Zeta Potential.** In this experimental research study, we synthesized DG4-polox-coumarin NPs. To define them, a particular method was used as shown in Figure 2. SEM was used to characterize the shape of DG4-polox-coumarin NP, as shown in Figure 2a. The image obtained from SEM shows that the particles have a spherical shape and a smooth outer surface.

The size distribution analysis showed that the average diameter of DG4-polox-coumarin NP was  $97.81 \pm 0.243\text{ nm}$  (Figure 2b). The polydispersity of the representative sample was determined by DLS analysis, i.e., the polydispersity index was 0.336. The size reproducibility was acceptable. The formulation of DG4-polox-coumarin NP had a zeta potential of  $-5.15 \pm 9.16\text{ mV}$  (Figure 2c). From the above result, it can be concluded that the formulations of DG4-polox-coumarin NP have excellent stability. The zeta potential shows repulsion between similarly charged neighboring particles in the dispersion, indicating that the drug charge affects the zeta potential.

**2.3. Estimation of Entrapment Efficiency.** DG4-polox-coumarin NPs have a hydrophobic interior and a hydrophilic surface. The formulation exhibited an increased entrapment efficiency of  $61.61 \pm 1.32\%$ . The amount of drug loaded was significantly higher in DG4-polox-coumarin NP. The results indicate that DG4-polox has a higher ability to encapsulate

coumarin. This view accelerates the overall driving force of loading (hydrophobic and electrostatic interaction). One of the probable reasons for the improvement of drug efficiency was observed. A similar result was reported in a previous study on drug entrapment efficiency.<sup>18</sup>

**2.4. In Vitro Biocompatibility Study.** The MTT test was used to determine the cytotoxicity of the final formulation to establish and confirm the biocompatibility of the drug product and excipients. The results of this evaluation are shown in Figure 3a. In an in vitro cell culture system, the biosafety of DG4-polox-coumarin conjugate NP was evaluated using two cell line models: A549 and HEK293. The results of the study showed that all selected cell lines exhibited cell viability between 95 and 99%. The experimental results showed that the newly synthesized DG4-polox-coumarin NP did not inhibit cell growth. According to the results of the study, the toxicity of the DG4-polox-coumarin conjugate NP was relatively low, and their biocompatibility was excellent. The conjugates of DG4-polox-coumarin NPs have high potential for use as in vivo antibacterial therapy due to their low toxicity and good biocompatibility.

**2.5. In Vitro Hemolysis.** As shown in Figure 3b, DG4-polox-coumarin NP was tested with fresh sheep blood at various concentrations to determine the percentage of hemolysis. Hemolysis rates were very low, indicating that DG4-polox-coumarin NP solutions up to 250  $\mu\text{g}/\text{mL}$  have excellent blood compatibility and are suitable for intravenous injection. As a result of the treatment, the hemolysis rate is extremely low, indicating that the administration of the drug is hemocompatible. Compared to coumarin, DG4-polox-coumarin NPs were found to have lower toxicity. This could be due to the fact that the drug is protected in a biocompatible dendritic environment that prevents the drug from coming into direct contact with cells.

**2.6. In Vitro Drug Release.** Figure 4a,b shows the results of the release study under three different conditions: acidic, neutral, and alkaline. The in vitro release behavior can be used to determine how chemical and biochemical factors affect the release of coumarin from DG4-polox-coumarin NPs at different pH values. At a pH of 1.2, the cumulative percent release of coumarin was  $47.26 \pm 1.47$  (2 h),  $79.36 \pm 2.10$  (4 h), and  $94.16 \pm 3.46$  (6 h). At pH 6.0, drug release was  $24.24 \pm 0.06$  (2 h),  $47.26 \pm 1.44$  (4 h),  $72.23 \pm 2.86$  (6 h), and  $93.26 \pm 3.74$  (12 h). At pH 7.4, drug release was  $12.09 \pm 0.60$  (2 h),  $28.99 \pm 1.44$  (4 h),  $57.26 \pm 2.86$  (6 h),  $74.89 \pm 3.74$  (12 h), and  $83.26 \pm 4.36$  (24 h). In this in vitro drug release study, explosive release of DG4-polox-coumarin NPs was observed in all three cases within minutes of the release study using the dialysis bag method. Simultaneous release of the payloads (under acidic conditions) and medially delayed release (at intermediate pH) were observed. The release is prolonged under alkaline conditions, suggesting a combined effect of pH-dependent conformational changes in dendritic architects by protonation. A similar in vitro release pattern under different pH conditions was reported by Tekade et al.<sup>18</sup> There is a possibility that sequestration of coumarin in the core of the newly modified hybrid polymer is responsible for the sustained release of coumarin. To ensure that the drug molecules were not restricted in their diffusion across the dialysis membrane during the release phase, the release of free coumarin was studied. Free coumarin was found to be released rapidly, reaching a peak concentration of more than 80% of the total concentration in the first 5 h after administration. The process of coumarin release from the core of a modified polymer involves several steps. These steps include

association with the polymer matrix, release by polymer degradation, solubilization, and diffusion through microchannels already present in the polymer matrix or formed by erosion in the polymer matrix. The release of coumarin from DG4-polox-coumarin NP clearly shows that modification plays a role in altering the release profile of the encapsulated active ingredient.

**2.7. In Vitro Antibacterial Activity.** Antibacterial activity against MRSA was tested in vitro. The results are given in Table 1. Compared to coumarin alone, DG4-polox-coumarin nano-

**Table 1. Comparative In Vitro Antibacterial Activity of Pure Coumarin and DG4-Polox-Coumarin NPs against MRSA Bacteria**

compound	MIC ( $\mu\text{g}/\text{mL}$ )	
	24 h	48 h
dendrimer G4 nanoparticle	$5 \mu\text{M}^{20}$	
bare coumarin	4.17	4.87
DG4-polox-coumarin NPs	1.12	1.14

particles had stronger antibacterial activity. The results speak to the range of nanoscale and increased surface area and indicate changes in properties that occur only at the nanoscale. Compared to pure coumarin, this formulation showed much stronger antibacterial activity. In general, the antibacterial activity of DG4-polox-coumarin nanoparticles against MRSA is much greater than that of the pure form. Interestingly, an improvement in MIC was observed for DG4-polox-coumarin nanoparticles. This could be due to the small size, high EE, and continuous slow release of drug resulting in the continuous delivery of lethal concentrations of antibiotics to bacteria over long periods of time. Thus, it is possible to completely eliminate the bacteria.<sup>19</sup> The improved activity could also be due to the small size of DG4-polox-coumarin, which increases the surface-to-volume ratio and enhances drug entrapment efficiency, leading to better penetration and uptake. Thus, the in vitro studies confirmed the ability of DG4-polox-coumarin to enhance the activity of coumarin against MRSA after its complexation with DG4-polox-coumarin.

**2.8. Bactericidal Time Kill Kinetics.** Figure 5 shows the microbiological mortality rate of the NPs of naked coumarin and DG4-polox-coumarin. We selected a dose five times higher than the MIC for each treatment and incubated the samples at 37 °C

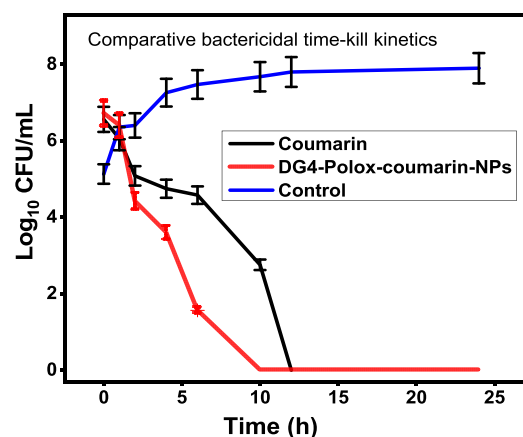


**Figure 5. Comparative bacterial time-kill kinetics of coumarin and DG4-polox-coumarin NP against MRSA.**

for 24 h. Compared with coumarin alone, DG4-polox-coumarin NP had a more rapid bactericidal effect, decreasing by three logarithms after 12 h. A bactericidal effect followed after 24 h. The die-off rate caused by coumarin is comparable to that documented in the scientific literature. This could lead to faster clearance of bacteria in the blood, which would reduce the duration of treatment and the amount of drug required for effective therapy.

**2.9. Stability Study.** The new formulations of DG4-polox-coumarin NP were tested for stability for 1 month at room temperature (RT) and 4 °C. The stability of the formulation was evaluated by % EE, PDI, and ZP, and the results are revealed in Table 2. DG4-polox-coumarin NP was stable for 1 month at 4

**Table 2. Effects of Storage Conditions on the Physics and Chemical Properties of the Formulation of DG4-Polox-Coumarin NP at Ambient Temperature**

days	size	ZP (mV)	EE%
0	97.81 ± 0.243	-5.15 ± 9.16	61.61 ± 1.32
15	99.20 ± 4.22	-9.2 ± 6.27	59.03 ± 2.43
30	102 ± 5.01	-10.2 ± 4.34	63.05 ± 3.45

°C ( $P$  value > 0.05), and no physical changes were observed in the formulation. After 15 days at room temperature (RT), the size and zeta potential changed slightly ( $P$  value > 0.05). This indicates that physical stability was achieved only during the 15 days. At room temperature, the instability of the formulation of DG4-polox-coumarin NP may be related to non-Fickian release mechanisms. The interaction with the aqueous medium may have caused the structural changes in the formulation of DG4-polox-coumarin NP.

### 3. MATERIALS AND METHODS

**3.1. Materials.** Coumarin was obtained from Koch Light Laboratories Limited, Saudi Arabia. Sodium phosphate dibasic dehydrate, 14,000 Da, and poloxamer were obtained from (Sigma-Aldrich, India). MTT and DMSO were obtained from Merck Chemicals, Germany. Mueller–Hinton agar (MHA), Mueller–Hinton broth (MHB), and nutrient broth were purchased from HiMedia Laboratories. Double-distilled water (DD) was used throughout the experiment. Because the other chemicals and solvents were of analytical purity, they did not require additional purification prior to use.

**3.2. Infrared Spectral Analysis.** Infrared spectroscopy, one of the most important analytical methods, provides a sensitive probe for the detection of certain functional groups in polymers and drugs.<sup>21,22</sup> The interaction of functional groups in chemical molecules with infrared light is monitored by infrared spectroscopy. This interaction results in predictable vibrations that provide a typical "fingerprint" of the chemical or biological compounds present in the sample. FTIR spectra (PerkinElmer FT-IR) were used to determine drug–carrier interactions in the physical mixture. In the course of four scans, spectra in the spectral range of 500–4000  $\text{cm}^{-1}$  were recorded in absorption mode IR with a resolution of 2  $\text{cm}^{-1}$ . The FTIR spectra of the pure drug and the physical combination were compared to verify the presence of drug–polymer interactions or to identify the change in the position of the drug functional group.

**3.3. Synthesis of Dendrimer G4-Poloxamer Conjugates.** To obtain dendrimer-G4-poloxamer conjugates, we followed the procedure with slight modifications. In the first step, we activated 2 g of poloxamer in 10 mL of dichloromethane

(DCM) according to the procedure described by Dung et al.<sup>23</sup> To prepare dendrimer G4-poloxamer conjugates, an appropriate amount of 10% activated poloxamer in methanol was transferred dropwise to a flask containing 100 mg of PAMAM G4 in 10 mL buffer (pH 7.5) at 40 °C.

**3.4. Preparation of Coumarin-Loaded Nanoparticles.** Coumarin-loaded dendrimer G4-poloxamer nanoparticles, also known as DG4-polox-coumarin-NP, were produced employing an evaporation method of the emulsification solvent with a few minor modifications.<sup>24</sup> After dissolving a measured amount of coumarin in 10 mL of water, a measured amount of dendrimer G4-poloxamer conjugates was added to the mixture, and then the whole was heated at 85 °C for half an hour with constant stirring. After an initial incubation period of 30 min, the resulting mixture was allowed to evaporate with constant magnetic stirring at 50 rpm with a Teflon ball. This was done to remove the organic solvent and harden the particles. Each formulation was made in triplicate during the process.

**3.5. Physicochemical Characterization of Coumarin-Loaded Dendrimer G4-Poloxamer Nanoparticles.** After dispersing the formulation in distilled water, the particle size, the polydispersity index (PDI), and the zeta size ( $n = 3$ ) were determined using the Zetasizer (Nano ZS, Malvern instrument, UK). Field-emission scanning electron microscopy (FE-SEM, Jeol, India) was used to determine the morphology and shape of NPs.

**3.6. Estimation of Entrapment Efficiency.** To maximize the effectiveness of the capture procedure, the samples were accurately weighed before being dissolved in methanol at a concentration of 1  $\text{mg mL}^{-1}$ . The resulting mixture was incubated for 24 h using Teflon beads and slow magnetic stirring (50 rpm). The dialysis preparation was used in the inclusion assay performed.<sup>25</sup> To remove the free drug from the formulation, a certain amount of the formulation was placed in a cellulose dialysis bag (MWt CO 1000 Da, Sigma, USA) and incubated for 30 min with 20 mL of methanol under sinking conditions. This was followed by the spectrophotometric determination of the free drug at a maximum wavelength of 360 nm. The following calibration concentrations were used to generate the coumarin calibration curve: 1–10  $\mu\text{g mL}^{-1}$ . After curve fitting was completed to generate the regression equation, the coumarin content was calculated relative to the respective absorbance using max at 360 nm. After noting the absorbance, we used it to calculate the concentration of the indirectly included drugs. The percentage of EE remained established on eq 1.

$$\%EE = \frac{(\text{total amount of coumarin} - \text{amount of coumarin in supernatant})}{(\text{total amount of coumarin})} \times 100 \quad (1)$$

**3.7. In Vitro Biocompatibility Study.** Using the MTT assay described in the previously described methods, the biocompatibility of coumarin-loaded dendrimer G4 poloxamer nanoparticles (DG4-polox-coumarin NP) was investigated in two different cell lines, basal epithelial cells (A549) and embryonic kidney cells (HEK-293).<sup>26</sup> Cells were seeded in 96-well culture plates at a density of 10,000 cells per well. The plates were then placed in an incubator at 37 °C for 24 h to promote cell adhesion. The cells were then treated with DG4-polox-coumarin NP at various concentrations ranging from 0 to 100  $\mu\text{g/mL}$ . After completion of 24 h, 20  $\mu\text{L}$  of MTT solution (5

mg/mL in PBS) was added to the cells and incubated for an additional 4 h at 37 °C. In the end, the medium was replaced with 100  $\mu$ L dimethyl sulfoxide (DMSO) and incubated at 37 °C for 10 min. The % cell viability remained designed according to eq 2.

$$\% \text{cell viability} = \frac{(A_{540 \text{ nm treated cells}})}{(A_{540 \text{ nm untreated cells}})} \times 100 \quad (2)$$

**3.8. In Vitro Hemolysis Activity.** The biocompatibility of the nanoslides was further determined by hemolytic analysis of the blood, which was followed by adaptation of the slides according to described protocol.<sup>27,28</sup> A freshly obtained sample of sheep blood was centrifuged three times in an isotonic 0.1 M PBS solution (pH 7.4). To obtain the concentrations of 0.0, 50, 100, 150, 200, and 250  $\mu$ g/mL for each sample, the formulation of DG4-polox-coumarin NP was first diluted with 0.1 M PBS. An additional 0.2 mL of red blood cell suspension (RBC) was added to the 1.8 mL for each sample. The supernatant was obtained by centrifuging the samples after they had been incubated for 30 min at 37 °C. The supernatant was then collected and subjected to UV spectrophotometry at a maximum wavelength of 541 nm. The following equation was used to determine the degree of hemolysis:

$$\% \text{hemolysis} = \frac{(A_t - A_c)}{(A_x - A_c)} \times 100 \quad (3)$$

**3.9. In Vitro Drug Release.** A total of 100 mg of DG4-polox-coumarin NP was enclosed in a dialysis bag (MWCO 3000 Da) and placed in a buffer solution (pH 7.4). Throughout the experiment, the external phases were continuously stirred at a speed of 50 rpm and heated to 37 °C. At regular intervals, a 2 mL sample of the medium is taken and filtered through a 0.45  $\mu$ m membrane filter. The volume removed was replaced by an equal volume of new medium. By comparing the absorbance of DG4-polox-coumarin with the standard calibration curve, we were able to calculate the amount of DG4-polox-coumarin present in the sample. Each sample was analyzed three times, and the cumulative release profile was calculated. Using the following calculation, the cumulative release is calculated at each time point.

$$\text{CR}\% = (M_t/M_i) \times 100$$

where  $M_i$  and  $M_t$  are the initial amount of drug formulated and the amount of drug released at time  $t$ , respectively.

**3.10. In Vitro Antibacterial Activity.** **3.10.1. Minimum Inhibitory Concentration (MIC) Assay.** The broth micro-dilution method was used to test antibacterial activity in BAA-1683 strains, (MRSA) and results were evaluated according to previously established procedures.<sup>29,30</sup> The initial inoculum of these strains was grown in nutrient broth at 37 °C and 100 rpm for 18 h in a shaker incubator. The tested substances were serially diluted in MHB broth and then cultured for 24 h in a shaking incubator at 37 °C and 100 rpm with bacterial cultures containing  $5 \times 10^5$  colony forming units per mL (CFU/mL). On Mueller–Hinton Agar (MHA) plates, 10  $\mu$ L of serially diluted solutions were detected. It was incubated for the next 24 h. MIC was determined for each sample by looking for the location where there was no visible bacterial growth. Each sample was repeated three times.

**3.10.2. Bactericidal Time Kill Kinetics.** Bacterial time-kill assays were performed according to CLSI guideline M26-A.<sup>29</sup> MRSA culture in MHB was diluted with phosphate buffer to  $5 \times$

$10^5$  CFU/mL. Coumarin powder and DG4-polox-coumarin NP were added at concentrations equal to 5 times the MIC result. Sterile water was added to the test samples to this bacterial broth to serve as a negative control. The viability of the bacterial cells was continuously monitored for 24 h. Samples were collected at specific time intervals, serially diluted in PBS, and plated in triplicate on MHA plates. The incubation was carried out overnight at 37 °C, and after incubation, the development of bacteria estimated the colonies on the plates.

**3.11. Physical Stability.** A short-term change in physical stability was also performed to test how temperature affects DG4-polox-coumarin NP. According to the protocols approved by the International Conference on Harmonization, the DG4-polox-coumarin NP formulations were kept at a temperature of 4 °C and room temperature for a period of 0, 15, and 30 days, and the samples were analyzed for their physicochemical properties at each of these intervals.<sup>31</sup> It was analyzed for all visible changes, including precipitation, turbidity, crystallization, color, particle size, PDI, and ZP.

## 4. CONCLUSIONS

The problem of resistance development by various intracellular pathogens and the continuous spread of infections to cells, tissues, and organs leads to recurrent infections. To combat MRSA, we synthesized DG4-polox-coumarin NP. Incorporation of coumarin into DG4-polox conjugates showed efficient encapsulation and prolonged drug release. DG4-polox-coumarin NPs showed minimal toxicity profile, good performance in terms of encapsulation efficiency, and sustained regulated drug release compared to naked NPs. In particular, DG4-polox-coumarin NPs represent a promising and useful technique for stable, safe, and efficient delivery of coumarin with enhanced antibacterial activity, thereby addressing current public health challenges related to antimicrobial drug resistance.

## AUTHOR INFORMATION

### Corresponding Author

Ahmed I. Foudah – Department of Pharmacognosy, College of Pharmacy, Prince Sattam Bin Abdulaziz University, Al-Kharj 11942, Saudi Arabia; [orcid.org/0000-0002-8020-3689](https://orcid.org/0000-0002-8020-3689); Email: [a.foudah@psau.edu.sa](mailto:a.foudah@psau.edu.sa), [ahmedfoudah11@gmail.com](mailto:ahmedfoudah11@gmail.com)

### Authors

Mohammed H. Alqarni – Department of Pharmacognosy, College of Pharmacy, Prince Sattam Bin Abdulaziz University, Al-Kharj 11942, Saudi Arabia

Samir A. Ross – National Center for Natural Products Research, School of Pharmacy and Department of Biomolecular Sciences, School of Pharmacy, The University of Mississippi, University, Oxford, Mississippi 38677, United States; [orcid.org/0000-0002-3807-1299](https://orcid.org/0000-0002-3807-1299)

Aftab Alam – Department of Pharmacognosy, College of Pharmacy, Prince Sattam Bin Abdulaziz University, Al-Kharj 11942, Saudi Arabia

Mohammad Ayman Salkini – Department of Pharmacognosy, College of Pharmacy, Prince Sattam Bin Abdulaziz University, Al-Kharj 11942, Saudi Arabia

Piyush Kumar – Department of Chemistry, Indian Institute of Technology, Jammu 181221, India

Complete contact information is available at:

<https://pubs.acs.org/10.1021/acsomega.2c03659>

## Funding

This research was funded by the Deputyship for Research & Innovation, Ministry of Education in Saudi Arabia, through the project number-IF-PSAU-2021/03/17778, and The APC was funded by IF-PSAU.

## Notes

The authors declare no competing financial interest.

## REFERENCES

- (1) Hu, D.; Zou, L.; Li, B.; Hu, M.; Ye, W.; Ji, J. Photothermal Killing of Methicillin-Resistant Staphylococcus Aureus by Bacteria-Targeted Polydopamine Nanoparticles with Nano-Localized Hyperpyrexia. *ACS Biomater. Sci. Eng.* **2019**, 5169.
- (2) Doyle, M. E.; Hartmann, F. A.; Wong, A. C. L. Methicillin-Resistant Staphylococci: Implications for Our Food Supply? *Anim. Health Res. Rev.* **2012**, 157.
- (3) Singh, S.; Aldawsari, H. M.; Alam, A.; Alqarni, M. H. S.; Ranjan, S.; Kesharwani, P. Synthesis and Antimicrobial Activity of Vancomycin–Conjugated Zinc Coordination Polymer Nanoparticles against Methicillin-Resistant Staphylococcus Aureus. *J. Drug Deliv. Sci. Technol.* **2022**, No. 103255.
- (4) de Kraker, M. E. A.; Stewardson, A. J.; Harbarth, S. Will 10 Million People Die a Year Due to Antimicrobial Resistance by 2050? *PLoS Med.* **2016**, No. e1002184.
- (5) Frieden, T. *Antibiotic Resistance Threats in the United States*, 2013 | Antibiotic/Antimicrobial Resistance Report. *US Dep Heal Hum Serv Centers Dis Control Prev* 2013.
- (6) El-Halfawy, O. M.; Czarny, T. L.; Flannagan, R. S.; Day, J.; Bozelli, J. C.; Kuiuack, R. C.; Salim, A.; Eckert, P.; Epand, R. M.; McGavin, M. J.; Organ, M. G.; Heinrichs, D. E.; Brown, E. D. Discovery of an Antivirulence Compound That Reverses  $\beta$ -Lactam Resistance in MRSA. *Nat. Chem. Biol.* **2020**, 143.
- (7) Cabrera, R.; Fernández-Barat, L.; Motos, A.; López-Aladid, R.; Vázquez, N.; Panigada, M.; Álvarez-Lerma, F.; López, Y.; Muñoz, L.; Castro, P.; Vila, J.; Torres, A. Molecular Characterization of Methicillin-Resistant Staphylococcus Aureus Clinical Strains from the Endotracheal Tubes of Patients with Nosocomial Pneumonia. *Antimicrob. Resist. Infect. Control* **2020**, 1.
- (8) Singh, S.; Numan, A.; Cinti, S. Point-of-Care for Evaluating Antimicrobial Resistance through the Adoption of Functional Materials. *Anal. Chem.* **2022**, 26.
- (9) Vukomanovic, M.; del Mar Cendra, M.; Baelo, A.; Torrents, E. Nano-Engineering Stable Contact-Based Antimicrobials: Chemistry at the Interface between Nano-Gold and Bacteria. *Colloids Surf., B* **2021**, No. 112083.
- (10) Lakhundi, S.; Zhang, K. Methicillin-Resistant Staphylococcus Aureus: Molecular Characterization, Evolution, and Epidemiology. *Clin. Microbiol. Rev.* **2018**, No. e00020.
- (11) Smyth, T.; Ramchandran, V. N.; Smyth, W. F. A Study of the Antimicrobial Activity of Selected Naturally Occurring and Synthetic Coumarins. *Int. J. Antimicrob. Agents* **2009**, 421.
- (12) Alnufaie, R.; Kc, H. R.; Alsup, N.; Whitt, J.; Chambers, S. A.; Gilmore, D.; Alam, M. A. Synthesis and Antimicrobial Studies of Coumarin-Substituted Pyrazole Derivatives as Potent Anti-Staphylococcus Aureus Agents. *Molecules* **2020**, 2758.
- (13) Qu, D.; Hou, Z.; Li, J.; Luo, L.; Su, S.; Ye, Z.; Bai, Y.; Zhang, X.; Chen, G.; Li, Z.; Wang, Y.; Xue, X.; Luo, X.; Li, M. A New Coumarin Compound DCH Combats Methicillin-Resistant Staphylococcus Aureus Biofilm by Targeting Arginine Repressor. *Sci. Adv.* **2020**, No. eaay9597.
- (14) da Cunha, M. G.; de Cássia Orlandi Sardi, J.; Freires, I. A.; Franchin, M.; Rosalen, P. L. Antimicrobial, Anti-Adherence and Antibiofilm Activity against Staphylococcus Aureus of a 4-Phenyl Coumarin Derivative Isolated from Brazilian Geopropolis. *Microb. Pathog.* **2020**, No. 103855.
- (15) Hu, Y.; Hu, C.; Pan, G.; Yu, C.; Ansari, M. F.; Yadav Bheemanaboina, R. R.; Cheng, Y.; Zhou, C.; Zhang, J. Novel Chalcone-Conjugated, Multi-Flexible End-Group Coumarin Thiazole Hybrids as Potential Antibacterial Repressors against Methicillin-Resistant Staphylococcus Aureus. *Eur. J. Med. Chem.* **2021**, No. 113628.
- (16) Hu, C. F.; Zhang, P. L.; Sui, Y. F.; Lv, J. S.; Ansari, M. F.; Battini, N.; Li, S.; Zhou, C. H.; Geng, R. X. Ethylenic Conjugated Coumarin Thiazolidinediones as New Efficient Antimicrobial Modulators against Clinical Methicillin-Resistant Staphylococcus Aureus. *Bioorg. Chem.* **2020**, No. 103434.
- (17) Singh, S.; Numan, A.; Somaily, H. H.; Gorain, B.; Ranjan, S.; Rilla, K.; Siddique, H. R.; Kesharwani, P. Nano-Enabled Strategies to Combat Methicillin-Resistant Staphylococcus Aureus. *Mater Sci Eng C* **2021**, No. 112384.
- (18) Tekade, R. K.; Dutta, T.; Gajbhiye, V.; Jain, N. K. Exploring Dendrimer towards Dual Drug Delivery: PH Responsive Simultaneous Drug-Release Kinetics. *J. Microencapsulation* **2009**, 287.
- (19) Hassan, D.; Omolo, C. A.; Gannimani, R.; Waddad, A. Y.; Mocktar, C.; Rambharose, S.; Agrawal, N.; Govender, T. Delivery of Novel Vancomycin Nanoplexes for Combating Methicillin Resistant Staphylococcus Aureus (MRSA) Infections. *Int. J. Pharm.* **2019**, 143.
- (20) Felczak, A.; Zawadzka, K.; Wronska, N.; Janaszewska, A.; Klajnert, B.; Bryszewska, M.; Appelhans, D.; Voit, B.; Lisowska, K. Enhancement of Antimicrobial Activity by Co-Administration of Poly(Propylene Imine) Dendrimers and Nadifloxacin. *New J. Chem.* **2013**, 4156.
- (21) Beć, K. B.; Grabska, J.; Huck, C. W. Near-Infrared Spectroscopy in Bio-Applications. *Molecules* **2020**, 383.
- (22) Beć, K. B.; Grabska, J.; Huck, C. W. Biomolecular and Bioanalytical Applications of Infrared Spectroscopy – A Review. *Anal. Chim. Acta* **2020**, 150.
- (23) Dung, T. H.; Kim, J.; Kim, M. S.; Kim, J. S.; Yoo, H. Preparation and Biophysical Characterization of Pluronic F127-Dendrimer Conjugate as a Delivery Agent of Antisense Oligonucleotides. *Int. J. Nanoscience and Nanotechnology*; 2008, DOI: 10.1166/jnn.2008.1219.
- (24) Sonawane, S. J.; Kalhapure, R. S.; Rambharose, S.; Mocktar, C.; Vepuri, S. B.; Soliman, M.; Govender, T. Ultra-Small Lipid-Dendrimer Hybrid Nanoparticles as a Promising Strategy for Antibiotic Delivery: In Vitro and in Silico Studies. *Int. J. Pharm.* **2016**, 1.
- (25) Kesharwani, P.; Tekade, R. K.; Jain, N. K. Formulation Development and in Vitro-in Vivo Assessment of the Fourth-Generation PPI Dendrimer as a Cancer-Targeting Vector. *Nano-medicine* **2014**, 2291.
- (26) Singh, S.; Alrobaian, M. M.; Molugulu, N.; Agrawal, N.; Numan, A.; Kesharwani, P. Pyramid-Shaped PEG-PCL-PEG Polymeric-Based Model Systems for Site-Specific Drug Delivery of Vancomycin with Enhance Antibacterial Efficacy. *ACS Omega* **2020**, 11935.
- (27) Garg, A. K.; Maddiboyina, B.; Alqarni, M. H. S.; Alam, A.; Aldawsari, H. M.; Rawat, P.; Singh, S.; Kesharwani, P. Solubility Enhancement, Formulation Development and Antifungal Activity of Luliconazole Niosomal Gel-Based System. *J. Biomater. Sci. Polym. Ed.* **2021**, 1009.
- (28) Yang, Z.; Hao, X.; Chen, S.; Ma, Z.; Wang, W.; Wang, C.; Yue, L.; Sun, H.; Shao, Q.; Murugadoss, V.; Guo, Z. Long-Term Antibacterial Stable Reduced Graphene Oxide Nanocomposites Loaded with Cuprous Oxide Nanoparticles. *J. Colloid Interface Sci.* **2019**, 13.
- (29) CLSI M26-A. Methods for Determining Bactericidal Activity of Antimicrobial Agents; Approved Guideline. CLSI Document M26-A. Pennsylvania, USA. *Clin. Lab. Stand. Inst.* **1999**.
- (30) Chung, S. H.; Cho, S.; Kim, K.; Lim, B. S.; Ahn, S. J. Antimicrobial and Physical Characteristics of Orthodontic Primers Containing Antimicrobial Agents. *Angle Orthod.* **2017**, 307.
- (31) Guy, R. C. International Conference on Harmonisation. In *Encyclopedia of Toxicology: Third Edition*; 2014, DOI: 10.1016/B978-0-12-386454-3.00861-7.